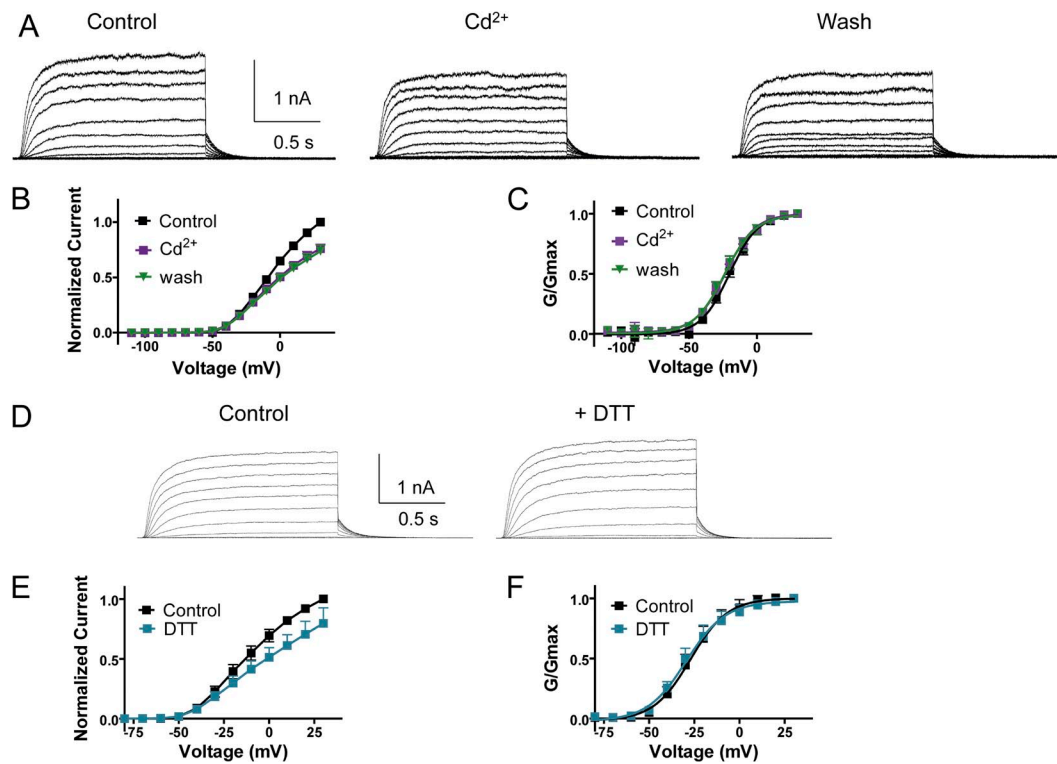
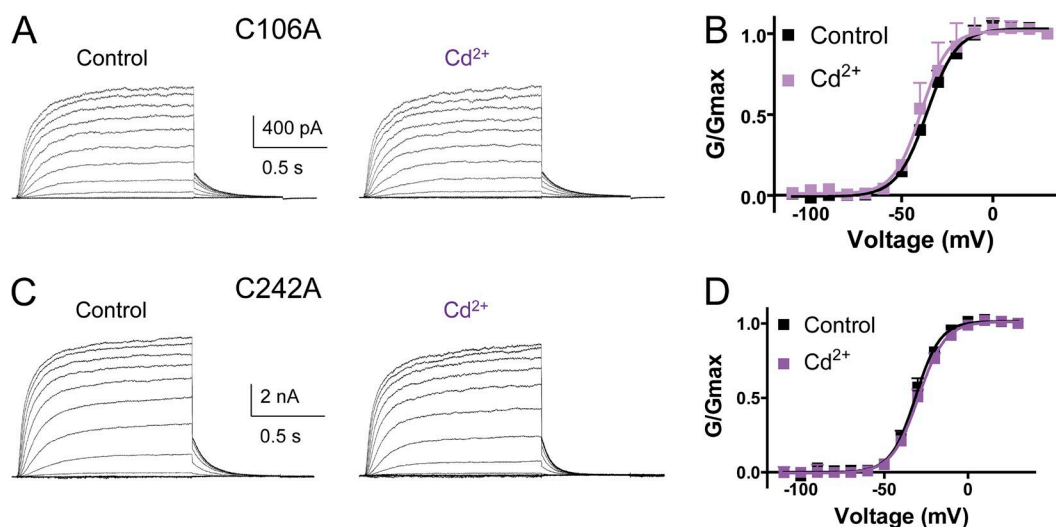
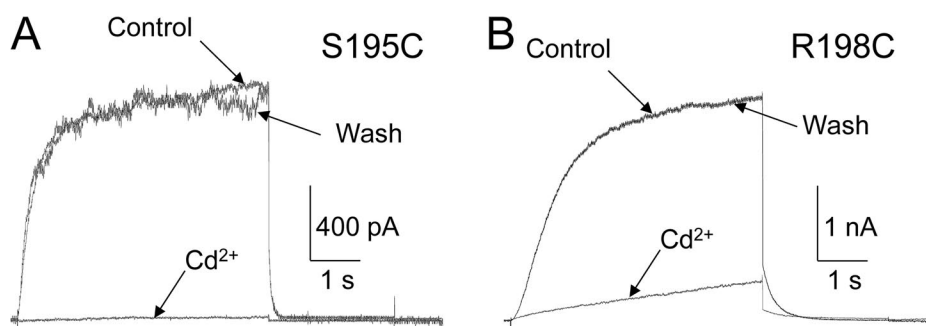


Gourgy-Hacohen et al., <http://www.jgp.org/cgi/content/full/jgp.201411221/DC1>

**Figure S1.** Effects of  $\text{Cd}^{2+}$  ions and DTT on WT KCNQ2 expressed in CHO cells. (A) Representative current traces of WT KCNQ2 in the absence (control), presence, or after wash of  $100 \mu\text{M}$   $\text{Cd}^{2+}$  ions. Currents were evoked from a holding potential of  $-90 \text{ mV}$  by depolarizing steps from  $-110$  to  $30 \text{ mV}$  in  $10\text{-mV}$  increments and repolarized to  $-60 \text{ mV}$ . (B) Normalized current-voltage relations;  $n = 23$ . (C) Conductance-voltage relations;  $n = 23$ . (D) Representative current traces of WT KCNQ2 in the absence (control) or presence of  $100 \mu\text{M}$  DTT. Currents were evoked from a holding potential of  $-90 \text{ mV}$  by depolarizing steps from  $-80$  to  $30 \text{ mV}$  in  $10\text{-mV}$  increments and repolarized to  $-60 \text{ mV}$ . (E) Normalized current-voltage relations;  $n = 7$ . (F) Conductance-voltage relations;  $n = 7$ . Data were fitted to a single Boltzmann function. Error bars show mean  $\pm$  SEM.



**Figure S2.** Effects of Cd<sup>2+</sup> ions on endogenous KCNQ2 cysteine mutants C106A and C242A expressed in CHO cells. (A) Representative current traces of the KCNQ2 S1 mutant, C106A, in the absence or presence of 100 μM Cd<sup>2+</sup> ions. Currents were evoked from a holding potential of -90 mV by depolarizing steps from -110 to 30 mV in 10-mV increments and repolarized to -60 mV. (B) Conductance-voltage relations;  $n = 5$ . Data were fitted to a single Boltzmann function. (C) Representative current traces of the KCNQ2 S5 mutant, C142A, in the absence or presence of 100 μM Cd<sup>2+</sup> ions. Currents were evoked as in A. (D) Conductance-voltage relations;  $n = 6$ . Data were fitted to a single Boltzmann function. Error bars show mean  $\pm$  SEM.



**Figure S3.** Closed-state dependence of Cd<sup>2+</sup> inhibition of S195C and R198C mutants expressed in CHO cells. (A and B) Closed-state dependence of Cd<sup>2+</sup> inhibition of S195C and R198C mutant currents, respectively. Cells were preincubated for 5 min with 100 μM Cd<sup>2+</sup> at -90 mV. Then, current amplitude was measured at the first depolarizing pulse to 30 mV and compared in the same cell without Cd<sup>2+</sup> pretreatment (control).

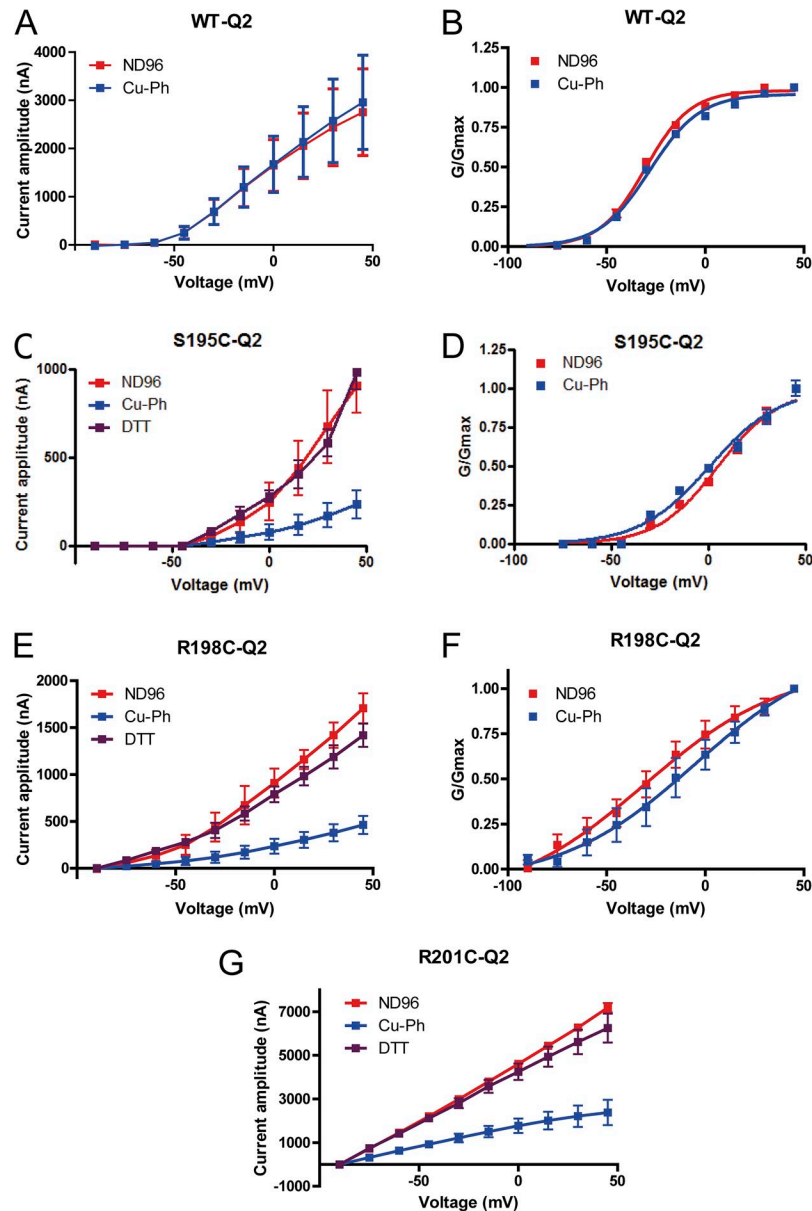


**Figure S4.** Effects of Cu-Phen on KCNQ2 S4 mutants S195C, R198C, and R201C expressed in *Xenopus* oocytes. (A and B) Current-voltage and conductance-voltage relations, respectively, of WT KCNQ2 in the absence (ND96) or presence of 100  $\mu$ M Cu-Phen;  $n = 10$ . (C and D) Current-voltage and conductance-voltage relations, respectively, of mutant S195C in the absence (ND96) or presence of 100  $\mu$ M Cu-Phen exposed in the closed state and after washout with 1 mM DTT. Oocytes were incubated for 2 min at  $-80$  mV in ND96 solution containing 100  $\mu$ M Cu-Phen and washed with ND96 for another 5 min at  $-80$  mV. Then, *Xenopus* oocytes were depolarized from  $-90$  to  $45$  mV in  $15$ -mV increments and repolarized at  $-60$  mV;  $n = 8$ . (E and F) Current-voltage and conductance-voltage relations, respectively, of mutant R198C in the absence (ND96) or presence of 100  $\mu$ M Cu-Phen exposed in the closed state and after washout with 1 mM DTT. Oocytes were incubated for 2 min at  $-80$  mV in ND96 solution containing 100  $\mu$ M Cu-Phen and washed with ND96 for another 5 min at  $-80$  mV. Then, *Xenopus* oocytes were depolarized from  $-90$  to  $45$  mV in  $15$ -mV increments and repolarized at  $-60$  mV;  $n = 7$ . (G) Current-voltage relations of mutant R201C in the absence (ND96) or presence of 100  $\mu$ M Cu-Phen exposed at  $-80$  mV and after wash-out with 1 mM DTT. Oocytes were incubated and depolarized as in C;  $n = 7$ . Error bars show mean  $\pm$  SEM.



**Figure S5.** Sequence alignments. (A) Pairwise sequence alignment between KCNQ2 (SwissProt accession no. O43526) and the chimeric Kv1.2–Kv2.1 K<sup>+</sup> channel (PDB accession no. 2R9R). This alignment was used in building the initial 3-D homology model of the open state of KCNQ2, with Kv1.2–Kv2.1 serving as a structural template. Underlined are counterpart amino acids whose C $\alpha$  atoms are aligned perfectly in three dimensions (see Structural modeling of the KCNQ2 channel open and closed states in Materials and methods in the main text). Helical segments are indicated as S1–S6 and the pore helix. (B) Sequences of the S4 voltage-sensor segments (light and dark magenta) of the various homology models built in this study. The underlined sequences (colored in dark magenta) correspond to 3<sub>10</sub> helices, whereas the residues colored in light magenta are folded as  $\alpha$  helices. C3, deep resting state; C2, intermediate resting state; C1, superficial resting state; O, open state. (C) Pairwise sequence alignment between the S6 segments of KCNQ2 and KcsA (SwissProt accession no. P0A334). Underlined are residues that line the ion channel pore, between the water-filled cavity and the activation gate (A317).